Vol. XVII, Nº 2, Diciembre (2009)
Matemáticas: 41–56

Matemáticas:
Enseñanza Universitaria

A numerical method to solve a nonlocal dispersive wave system

Juan Carlos Muñoz
Univesidad del Valle

Received Mar. 4, 2009 Accepted Aug. 11, 2009

Abstract

We use a spectral method to solve numerically a generalization of an integro-differential system proposed by Choi and Camassa [4] as a model to describe internal waves propagating at the interface of two immiscible inviscid fluids with different constant densities. The proposed numerical solver is able to capture well the dynamics of the solutions. The model is given in terms of the wave elevation η and the fluid velocity U. Furthermore, we show that each component of a solitary-like solution (η, U) of the system satisfies approximately a generalized Intermediate Long Wave equation, provided that nonlinear and dispersive effects are small.

Keywords: Coth transform, ILW equation, internal waves.

MSC(2000): Primary: 76B55 Secondary: 65T50

1 Introduction

In this paper we consider the integro-differential system written in dimensionless variables:

$$\eta_t - U_x + \alpha(\eta U^p)_x = 0, \tag{1}$$

$$U_t + \frac{\alpha}{p+1}(U^{p+1})_x - \eta_x = \beta\rho_r \mathcal{T}[U_{xt}], \tag{2}$$

subject to the initial conditions $\eta(x,0) = \eta_0(x), U(x,0) = U_0(x)$. Here α, β are small positive real parameters, $\rho_r > 1$ is a real constant, $p \geq 1$ is a positive integer, and $\mathcal{T}[.]$ denotes the coth transform operator on the strip of height h defined by

$$\mathcal{T}[f](x) = \frac{1}{2h} p.v. \int f(x') coth\Big(\frac{\pi(x'-x)}{2h}\Big) dx', \tag{3}$$

where $p.v.\int$ stands for the integration in the principal value sense. In case that $p = 1$, system above corresponds to a reduced one-dimensional model derived originally by Choi and Camassa [4] for describing the behavior of an internal wave propagating at the interface of two immiscible fluids with constant densities ρ_1, ρ_2 with $\rho_r = \rho_2/\rho_1 > 1$, contained at rest in a long channel with a horizontal rigid top and bottom, the lighter fluid forming a horizontal layer (of height h_1 and density ρ_1) above a layer of heavier fluid (of height h_2 and density ρ_2) (see Figure 1). In this context of application, the variable x denotes the spatial position, the variable t is time and the function $\eta(x,t)$ denotes the amplitude of the wave at the point x and time t measured with respect to the rest level of the two-fluid interface.

The function $U(x,t)$ represents the vertical mean of the first component of the fluid velocities within the fluid at the point x. The regime considered is such that the height of the upper layer h_1 is small compared to the typical wavelength L (i.e. weak dispersion $\beta << 1$) and the typical wave amplitude is small compared to h_1 (i.e. weak nonlinearity $\alpha << 1$). Internal waves, for example appear in the ocean when salt concentration and differences in temperature generate water stratification. The understanding of the interaction of internal waves with the bottom profile is important in the study of ocean and atmosphere dynamics and in improving weather forecasting processes.

The system (1)-(2) with $p = 1$ was generalized by Choi and Camassa in [5] to a regime where the weak nonlinearity assumption is removed. On the other hand, Ruiz and Nachbin [13] derived a reduced one-dimensional fully nonlinear model for the evolution of internal waves over an arbitrary bottom topography which generalizes the one proposed by Choi and Camassa [4], [5] for the flat bottom case, in the same physical settings. Choi and Camassa [4] solved numerically system (1)-(2) only in the particular case that $p = 1$. They used a pseudospectral method in space and the time evolution was performed by a fourth-order Runge-Kutta integration scheme.

In this work we show that for weakly nonlinear, weakly dispersive unidirectional waves (i.e. α and β small), system (1)-(2) reduces asymptotically to a well known unidirectional model: the generalized Intermediate Long Wave equation (henceforth called ILW equation) for the fluid velocity $U(x,t)$:

$$U_t + U_x + \frac{\alpha(p+2)}{2} U^p U_x + \frac{\beta\rho_r}{2} \mathcal{T}[U_{xx}] = 0, \tag{4}$$

and a similar equation for the wave elevation $\eta(x,t)$. An important application of this result is that we can use equation (4) in order to find estimates of solitary-wavelike solutions of the original system (1)-(2) with $p \geq 1$, which has a more complicated structure. The equation (4) with $p = 1$ has been studied by Joseph [8], Kubota et al. [10] and by Albert et al. [2]. The global well-posedness of the initial-value problem for the ILW equation has been established by Abdelouhab et. al [1]. Recently Pelloni and Dougalis [12] introduced a spectral method to solve numerically the ILW equation ($p = 1$) and investigated the behavior of solitary-like solutions of this equation. The second contribution of the present work is to introduce a new spectral-type numerical solver which is capable of calculating approximations of solutions to the generalized system (1)-(2) with $p \geq 1$. It is based on the Fast Fourier Transform algorithm (FFT) [3] which makes easier the numerical treatment of the nonlocal term $\mathcal{T}[U_{xt}]$ which is present in the system. The time integration in this scheme is computed by using an inexpensive implicit-explicit type technique. Solutions in analytic form to the system (1)-(2) for arbitrary initial conditions are unknown and thus the numerical strategy is a valuable tool in the study of the full wave dynamics described by this model. We explore the properties of the numerical solver by using some approximations to

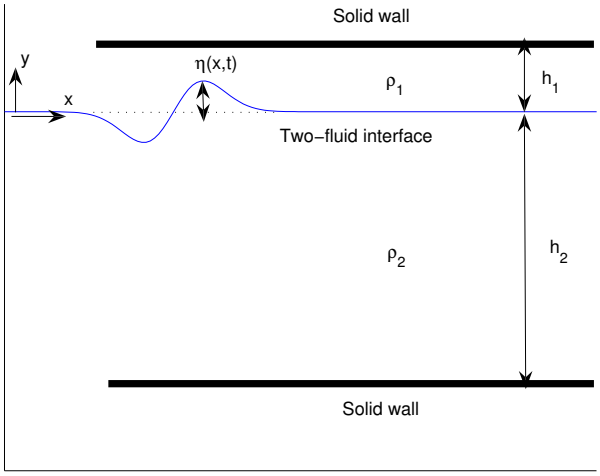

Figure 1: A typical internal wave propagating in a two-fluid system. The rest level of the system is indicated with dashed line. The system of two layers considered is constrained to a region limited by horizontal rigid lids located at the top and at the bottom.

solitary-like solutions of this system (with $p = 1$), in case that the wave velocity is close to 1. Some simulations are also conducted to analyze the behavior of solutions of system (1)-(2) as the nonlinear parameter α tends to zero. Other contribution of this paper is to show the application of the spectral approach to treat integro-differential models where the coth transform operator appears in both periodic and non-periodic spatial domains.

This work is organized as follows. In section 2 we show that the wave elevation $\eta(x,t)$ and the fluid velocity $U(x,t)$ satisfy approximately ILW-type equations provided that the parameters α and β are small and assuming that waves propagate at the interface in only one direction. In section 3 the numerical scheme is explained in detail. In section 4 we present some numerical simulations to test the ability of the solver to approximate solutions of the model equations. Finally, section 5 contains the conclusions of the work.

2 Solitary-wave solutions

We point out that a special linear operator (called coth transform) appears in the momentum equation (2). The coth transform is a singular integral operator defined in terms of the Cauchy principal value ($p.v.\int$) as:

$$\mathcal{T}f(x) = \frac{1}{2h} p.v. \int f(x') coth\Big(\frac{\pi(x'-x)}{2h}\Big) dx' \tag{5}$$

$$:= \frac{1}{2h} lim_{\epsilon \to 0} \int_{|x'-x| \geq \epsilon} f(x') coth\Big(\frac{\pi(x'-x)}{2h}\Big) dx'. \tag{6}$$

The main properties of this integral operator are the following:

$$\frac{d}{dx}\mathcal{T}[f](x) = \mathcal{T}[\frac{d}{dx}f](x), \tag{7}$$

$$\mathcal{T}[e^{ikx}](x) = i\coth(kh)e^{ikx}, \tag{8}$$

which are crucial in the computation of solutions of system (1)-(2) using a spectral-type method based on a Fourier basis. It is also important to point out that the coth transform is closely related to the classical Hilbert transform operator

$$\mathcal{H}f(x) := \frac{1}{\pi} p.v. \int \frac{f(x')}{x'-x} dx',$$

in the sense that $\lim_{h\to\infty} \mathcal{T}f(x) = \mathcal{H}f(x)$. The reader can find additional information on regard to the Hilbert and coth transforms and their properties in [6], [7], [11] and [14].

A *traveling wave solution* (η, U) with speed c of system (1)-(2) is a solution which can be written in the following form:

$$\eta(x,t) = \eta_c(\xi), \qquad U(x,t) = U_c(\xi), \qquad \xi = x - ct. \tag{9}$$

In case that the functions $\eta_c(\xi), U_c(\xi)$ and all their derivatives tend to zero when $|\xi| \to \infty$, the solution above is called a *solitary-wave or solitary-like solution* with velocity c. Note that a solitary-wave solution is an unidirectional translation of the initial profile (η_c, U_c).

Solitary waves have played an important role in the last decades in the study of dynamics of wave propagation in a broad set of applications such as, Fluid Dynamics, Optics, Acoustics, Oceanography and Weather Forecasting, among others. A recent spectacular application is the use of optical solitons in fibers as an efficient (reliable and fast) mean of long-distance communication [9]. Thus, the study of these type of solutions and their properties such as existence, uniqueness, orbital stability/instability under small perturbations and other properties is of great interest and has captured the attention of researchers who used both analytical and numerical means.

In case of system (1)-(2) it is difficult to find analytical expressions for solitary wave solutions, owing to the presence of the nonlocal operator $\mathcal{T}[.]$ in the system. To our knowledge it is an open problem to proof analytically whether solitary-wave solutions of this system exist for arbitrary wave velocity. However, asymptotic approximations for such type of solutions can be found. To show how it can be accomplished, let us suppose that we search for a solitary-wave solution (η, U) of system (1)-(2). Assume that the wave elevation is related with the fluid velocity in the following manner:

$$\eta = A_1 U + \alpha A_2 U^{p+1} + \beta A_3 \mathcal{T}[U_t], \tag{10}$$

where the constants A_1, A_2, A_3 will be determined bellow. This assumption incorporates the fact that the solution we are looking for propagates in only one direction. Also recall that we are interested in the case that the parameters α and β are small.

Substituting η given by equation (10) in system (1)-(2) we obtain the equations:

$$A_1 U_t + \alpha(p+1)A_2 U^p U_t + \beta A_3 \mathcal{T}[U_{tt}] - U_x + \alpha(p+1)A_1 U^p U_x = 0, \quad (11)$$
$$U_t + \alpha U^p U_x - A_1 U_x - \alpha(p+1)A_2 U^p U_x - \beta A_3 \mathcal{T}[U_{tx}] - \beta\rho_r \mathcal{T}[U_{tx}] = 0. \quad (12)$$

Observing the leading order terms in equation (12), it follows that

$$U_t = A_1 U_x + O(\alpha, \beta),$$

where $O(.)$ stands for the usual O-big notation. Thus, using this fact and multiplying by -1, equation (11) transforms into

$$-A_1 U_t - \alpha(p+1)A_1 A_2 U^p U_x - \beta A_1 A_3 \mathcal{T}[U_{tx}] + U_x - \alpha(p+1)A_1 U^p U_x = 0. \quad (13)$$

Now comparing each term in equations (12) and (13) we obtain that

$$-A_1 = 1, \quad \alpha - \alpha(p+1)A_2 = -\alpha(p+1)A_1 A_2 - \alpha(p+1)A_1, \quad (14)$$
$$-\beta A_3 - \beta\rho_r = -\beta A_1 A_3. \quad (15)$$

Therefore, we arrive at the appropriate values of the constants:

$$A_1 = -1, \quad A_2 = -\frac{p}{2(p+1)}, \quad A_3 = -\frac{\rho_r}{2}.$$

Hence the fluid velocity $U(x,t)$ satisfies the equation

$$U_t + U_x + \frac{\alpha(p+2)}{2} U^p U_x - \frac{\beta\rho_r}{2}\mathcal{T}[U_{tx}] = 0.$$

This equation implies that $U_t = -U_x + O(\alpha, \beta)$, and thus we see that the second order derivative ∂_{tx} can be interchanged by $-\partial_{xx}$. Therefore we yield that the fluid velocity U satisfies a generalized ILW equation:

$$U_t + U_x + \frac{\alpha(p+2)}{2} U^p U_x + \frac{\beta\rho_r}{2}\mathcal{T}[U_{xx}] = 0. \quad (16)$$

Also using that $U = -\eta + O(\alpha, \beta)$, we obtain that the wave elevation also satisfies a similar generalized ILW equation:

$$\eta_t + \eta_x - \frac{\alpha(p+2)(-1)^p}{2}\eta^p \eta_x + \frac{\beta\rho_r}{2}\mathcal{T}[\eta_{xx}] = 0. \quad (17)$$

In case that $p = 1$, it is known (see Joseph [8]) that the ILW equation (16) has a family of solitary-wave solutions with wave speed c close to 1, which can be expressed in analytical form:

$$U(x,t) = U_c(\xi) = \frac{A\cos^2\chi}{\cos^2\chi + \sinh^2\left(\frac{\xi}{\lambda_{ILW}}\right)}, \tag{18}$$

where $\xi = x - ct$,

$$A = \frac{4c_2}{hc_1}\chi\tan\chi, \quad \lambda_{ILW} = \frac{h}{\chi}, \quad c = 1 - \frac{2c_2}{h}\chi\cot(2\chi), \tag{19}$$

$$0 \le \chi < \pi/2, \quad c_1 = \frac{3}{2}\alpha, \quad c_2 = \frac{\beta\rho_r}{2}. \tag{20}$$

Now since $\eta = -U + O(\alpha,\beta)$ with α, β small, we arrive at

$$\eta(x,t) = \eta_c(\xi) = -\frac{A\cos^2\chi}{\cos^2\chi + \sinh^2\left(\frac{\xi}{\lambda_{ILW}}\right)}, \tag{21}$$

where all constants are the same as before.

The expressions (18) and (21) provide an approximation to a solitary-wave solution (η, U) of the original system (1)-(2) with $p = 1$, which was already derived by Choi and Camassa in a previous work [5]. Here we generalized their analysis for the case $p > 1$ obtaining the ILW equations (16)-(17).

3 The numerical scheme

In this section we introduce a numerical solver to approximate the solutions of system (1)-(2) with $p \ge 1$ integer, subject to the initial conditions $U(x,0) = U_0(x)$, $\eta(x,0) = \eta_0(x)$. To proceed, the spatial computational domain $[0, L]$ is discretized by N equidistant points, with spacing $\Delta x = L/N$. Then, we expand the unknowns U and η as a truncated Fourier series in space with time-dependent coefficients:

$$U(x,t) = \sum_j \widehat{U}_j(t)\phi_j(x), \tag{22}$$

$$\eta(x,t) = \sum_j \hat{\eta}_j(t)\phi_j(x)$$

with $\phi_j(x) = e^{iw_j x}$, $\quad w_j = \dfrac{2\pi j}{L}$, $\quad j = -N/2+1, ...0, ...N/2$. The time-dependent coefficients $\widehat{U}_j(t)$ for $j = -N/2+1, ...0, ...N/2$ are calculated by means of the equation

$$\widehat{U}_j(t) = \frac{1}{L}\int_0^L u(x,t)e^{-iw_j x}dx,$$

and similarly for $\hat{\eta}_j(t)$. Actually, this Fourier strategy allows us to seek approximations of solutions to system (1)-(2) on a periodic domain $[0, L]$. However, since in this paper we are mainly interested in solutions on $(-\infty, \infty)$ which decay rapidly to zero when $|x| \to \infty$, such as solitary waves and Gaussian-type initial data, we can take the length of the computational domain $L > 0$ large enough in order to the solution does not reach the computational boundaries $x = 0$, $x = L$. Thus we are able of computing the time evolution of solutions in these non-periodic problems.

Projecting the equations (1)-(2) with respect to the basis ϕ_j and the inner product

$$< f, g >= \frac{1}{T}\int_0^T f(x)\overline{g(x)}dx,$$

it yields that

$$< \eta_t, \phi_j > - < (U - \alpha\eta U^p)_x, \phi_j >= 0, \tag{23}$$

$$< U_t, \phi_j > + \frac{\alpha}{p+1} < (U^{p+1})_x, \phi_j > - < \eta_x, \phi_j >= \beta\rho_r < \mathcal{T}[U_{xt}], \phi_j > . \tag{24}$$

Now substituting the Fourier expansions (22) into equations (23)-(24) and using the ortogonal property of the basis ϕ_j, and integration by parts, we obtain

$$\hat{\eta}_j'(t) - iw_j P_j[(U - \alpha\eta U^p] = 0, \tag{25}$$

$$\widehat{U}_j'(t) + \frac{i\alpha w_j}{p+1} P_j[U^{p+1}] - iw_j\hat{\eta}_j = \beta\rho_r \sum_s iw_s\widehat{U}_s'(t) < \mathcal{T}[\phi_s], \phi_j >, \tag{26}$$

where $P_j[.]$ is the operator defined by

$$P_j[g] = \frac{1}{T}\int_0^T g(x)e^{-iw_j x}dx. \tag{27}$$

Here we used the property (7) which allow us to commute the derivative and coth transform operators.

Then using the property (8) of the coth transform $\mathcal{T}[.]$, system (25)-(26) reduces into

$$\hat{\eta}_j'(t) - iw_j P_j[(U - \alpha\eta U^p] = 0,$$

$$\widehat{U}_j'(t) + \frac{i\alpha w_j}{p+1} P_j[U^{p+1}] - iw_j\hat{\eta}_j = -\beta\rho_r w_j \coth(w_j h)\widehat{U}_j'(t).$$

Finally, we reach expressions for the Fourier coefficients of the unknowns U and η:

$$\hat{\eta}_j' = iw_j P_j[(U - \alpha\eta U^p], \tag{28}$$

$$\widehat{U}_j' = \frac{iw_j\hat{\eta}_j}{1 + \beta\rho_r w_j \coth(w_j h)} - \frac{i\alpha w_j P_j[U^{p+1}]}{(p+1)(1 + \beta\rho_r w_j \coth(w_j h))}. \tag{29}$$

Equations (28)-(29) can be considered as a system of Ordinary Differential Equations for each frequency w_j, which we discretize numerically by the following scheme:

$$\frac{\hat{\eta}_j^{(n+1)} - \hat{\eta}_j^{(n)}}{\Delta t} = \frac{3}{2} i w_j P_j[U - \alpha\eta U^p]^{(n)} - \frac{1}{2} i w_j P_j[U - \alpha\eta U^p]^{(n-1)}, \tag{30}$$

$$\frac{\widehat{U}_j^{(n+1)} - \widehat{U}_j^{(n)}}{\Delta t} = \frac{i w_j (\hat{\eta}_j^{(n+1)} + \hat{\eta}_j^{(n)})}{2(1 + \beta\rho_r w_j \coth(w_j h))} \; - \tag{31}$$

$$\frac{3 i\alpha w_j P_j[U^{p+1}]^{(n)}}{2(p+1)(1 + \beta\rho_r w_j \coth(w_j h))} + \frac{i\alpha w_j P_j[U^{p+1}]^{(n-1)}}{2(p+1)(1 + \beta\rho_r w_j \coth(w_j h))}.$$

Here Δt denotes the time step and $\widehat{U}_j^{(n)}$, $\hat{\eta}_j^{(n)}$, denote the numerical approximations of the Fourier coefficients $\widehat{U}_j(t)$, $\hat{\eta}_j(t)$, respectively, at time $t = n\Delta t$. Also the notation $P_j[g]^{(n)}$ means the value of $P_j[g]$ when g is evaluated at time $t = n\Delta t$. Observe that this scheme deals with three levels in the temporal evolution. To initiate the scheme we need the approximations of the pair solution (η, U) at two different levels of time. It is clear that the first level is given by the initial conditions $\eta_0(x), U_0(x)$. To compute the additional temporal level we may use, for instance, a single-step method to integrate equations (28)-(29).

We point out that the spectral strategy used above can be adapted without difficulty to treat other equations where the coth transform operator appears. For instance, using the same notation as above, the ILW-type equation (16) can be solved numerically by using the following scheme:

$$\frac{\widehat{U}_j^{(n+1)} - \widehat{U}_j^{(n)}}{\Delta t} = \frac{3}{2}\frac{i\alpha w_j (p+2)}{2(p+1)} P_j[U^{p+1}]^{(n)} - \frac{1}{2}\frac{i\alpha w_j (p+2)}{2(p+1)} P_j[U^{p+1}]^{(n-1)}$$

$$+ i(w_j + \frac{\beta\rho_r}{2} w_j^2 \coth(w_j h))\Big(\frac{\widehat{U}_j^{(n+1)} + \widehat{U}_j^{(n)}}{2}\Big).$$

4 Numerical experiments

In this section we present some numerical simulations by using the numerical solver introduced in this paper. In our experiments the computational domain is the interval $[0, 100]$, the number of FFT points in the spatial domain is 2^{10} and $\Delta t = 70/10000$ is the time step. In first place, let $p = 1$. To test the numerical method we will use the family of approximations of solitary-wave solutions of system (1)-(2) showed in section 2 (see equations (18) and (21)). Thus, we take the following initial conditions for η and U:

$$\eta(x, 0) = \eta_c(x - x_0), \qquad U(x, 0) = U_c(x - x_0), \tag{32}$$

and solve numerically system (1)-(2). We point out that the parameter x_0 appears in order to control the initial position of the soliton-like profile. In Figure 2

we compare the numerical solution with the approximations (18)-(21) computed at time $t = 70$. As expected, we see that they perfectly agree with excellent accuracy and neither numerical dispersion nor dissipation are evidenced in both the plot of the wave elevation $\eta(x,t)$ and the fluid velocity $U(x,t)$. The wave speed is approximately $c \approx 0.99018$ and the initial position of the solitary wave is $x_0 = 15$. This experiment also corroborates the accuracy of approximations (18)-(21) derived in section 2.

In Figure 3, we repeat the previous simulation for different solitary-wave's parameters. Now the wave speed results to be greater than 1, $c \approx 1.00256$ and see again that the profile obtained with the numerical method and the one corresponding to the approximate solitary-wavelike solution (18) and (21) coincide with good accuracy in the whole spatial domain as in the previous case.

In Figures 4 and 5 we plot the solutions $\eta(x,t), U(x,t)$ computed numerically taking the initial data in (32). It is evident from these plots that the solution maintains its shape as time evolves and the velocity of translation is a positive constant since the maximums of the surfaces describe a straight line with positive slope when projected onto the plane (x,t).

In Figure 6 we show that in general, the accuracy of approximations (18) and (21) deteriorates progressively when nonlinearity or system's dispersion (controlled by the parameters α and β, respectively) are too large. In this simulation for example, $\alpha = \beta = 0.1$ and see that the numerical solution (in solid line) breaks up into a main profile (propagating to the right) and a small amplitude component which propagates in opposite direction. Moreover there is a notorious discrepancy between the amplitude of the numerical solution and the approximate solitary-wave solution.

Next, we consider the case $p > 1$. This implies increasing the strength of nonlinearity in system (1)-(2). Thus, nonlinear effects in this system are expected to dominate dispersive ones. It is also important to point out that the parameter p appears inside the terms of order $O(\alpha, \beta)$ neglected in order to arrive at the ILW-type equations (16)-(17). Therefore it is expected that if the exponent p becomes larger, then the error of approximations (18) and (21) may increase. To analyze this fact, in Figure 7 we conduct an experiment where the nonlinear parameter is taken as $p = 2$. Observe that the shape of the numerical solution is not preserved and the solution profile tends to break.

The numerical scheme implemented is very useful for discovering properties of solutions for which there is at present no analytic proof and an exact solution is not available. For instance, it is interesting to study the behavior of solutions of system (1)-(2) as the nonlinear or dispersion parameters tends to zero. To illustrate this application of the numerical solver, we conduct a set of simulations in order to compare a nonlinear solution (denoted by η_α, U_α) of system (1)-(2), corresponding to $\alpha > 0$, with its linear counterpart $\eta_{linear}, U_{linear}$ (i.e. with $\alpha = 0$). We set $p = 3$, $\beta = 0.1$ and the initial conditions are Gaussian-type pulses

located at the position $x = 50$:

$$\eta(x,0) = e^{-2(x-50)^2}, \quad U(x,0) = -e^{-2(x-50)^2},$$

in all of the next experiments. In first place, let $\alpha = 0.3$. In Figures 8 and 9, we show the propagation of the initial Gaussian disturbance $\eta(x,0)$ and note that it gradually decomposes into a leading pulse which propagates to the right followed by a smaller oscillatory tail propagating to the left of the computational domain. In this simulation the difference between nonlinear and linear solutions is more notorious along the interval [60,90]. This is in accordance with our intuition since the nonlinear effects are intense with $\alpha = 0.3$.

We repeat in Figure 10 the simulation performed above, but now let us take the nonlinear coefficient smaller $\alpha = 0.1$. Remark that the discrepancies between the nonlinear and linear solutions are smaller than in the previous experiment. In Figure 11 we present the profile corresponding to the fluid velocity $U(x,t)$.

To see this issue more clearly, we now compute the nonlinear solution of system (1)-(2) corresponding to a set of values of the nonlinear parameter α. The initial data are the same Gaussian pulses as before, and other model's parameters are left unchanged. We use the discrete L^2-norm

$$\|\eta_\alpha - \eta_{linear}\| = \Big(\frac{L}{N}\sum_{j=1}^{N} |\eta_\alpha(j\Delta x,t) - \eta_{linear}(j\Delta x,t)|^2\Big)^{1/2}, \tag{33}$$

at time $t = 30$, for measuring the difference between the nonlinear solution η_α and the linear solution η_{linear} of system (1)-(2). Similarly for the case of the fluid velocity $U(x,t)$. The results are presented in Figure 12. From these experiments, we conjecture that at a fixed time t, the nonlinear solution η_α, U_α of system (1)-(2) approaches in the L^2-norm to the linearized solution as long as $\alpha \to 0$. To our knowledge, there is a lack of theory explaining this fact. The present computer simulations may be taken as a starting point for the development of an analytical theory on this regard.

5 Conclusions

In this paper we introduced a new numerical solver to approximate the solutions of the Cauchy problem associated to system (1)-(2) and showed that, in the regime of weak nonlinearity and weak dispersion (i.e. $\alpha << 1$, $\beta << 1$) each component of a solitary-like solution (η, U) of this system approximately satisfies a generalized ILW-type equation. In all computer simulations performed the numerical scheme proved to capture very well the dispersive and nonlinear nature of system (1)-(2). The main characteristics of the scheme are the following: low computational cost, it is easy to implement in a computer system and can be adapted without difficulty to solve other similar systems. Furthermore, the scheme can be used to

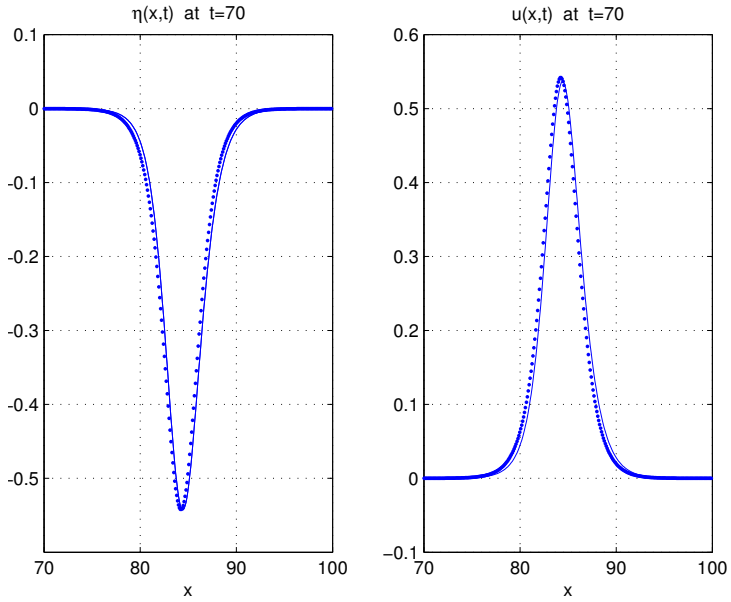

Figure 2: In points: approximate solitary wave solution (18)-(21). In solid line: solution obtained with the numerical solver. Model's parameters: $\chi = \pi/8$, $\rho_r = 2.5$, $\alpha = \beta = 0.01$, $h = 1$.

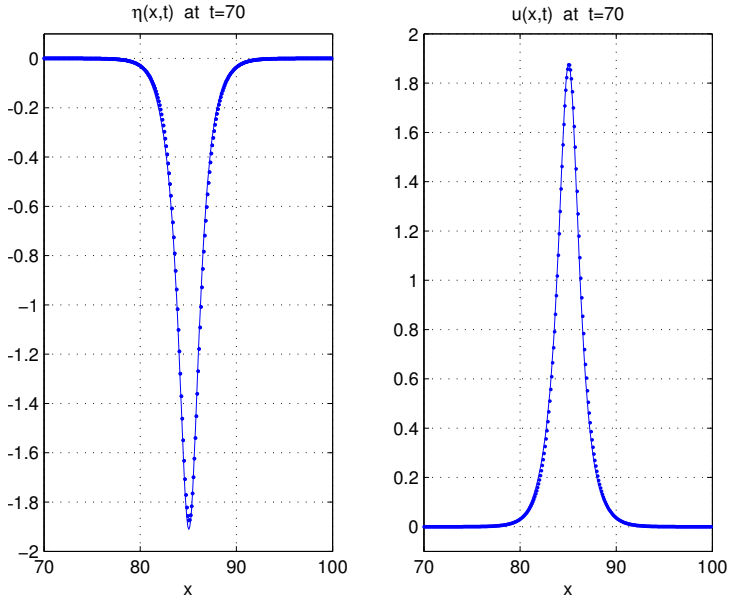

Figure 3: In points: approximate solitary wave solution (18)-(21). In solid line: solution obtained with the numerical solver. Model's parameters: $\chi = \pi/3.5$, $\rho_r = 2.5$, $\alpha = \beta = 0.01$, $h = 2$.

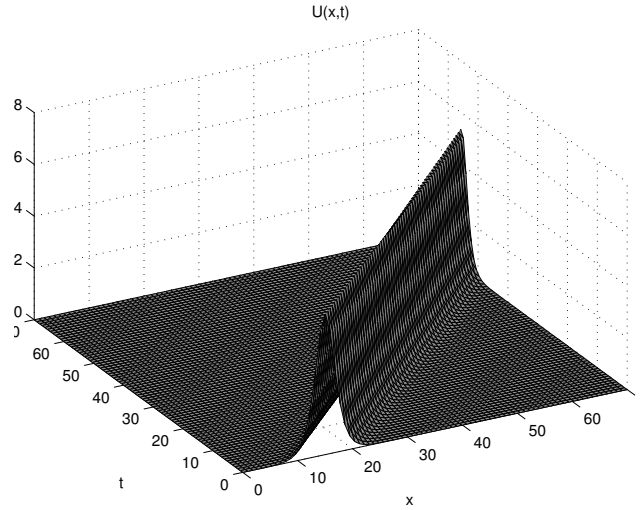

Figure 4: Solitary wave $U(x,t)$ as a function of x and t computed by using the numerical scheme. Model's parameters: $\alpha = \beta = 0.01$, $\chi = \pi/8$, $\rho_r = 2.5$, $h = 1$ and the wave speed is $c \approx 0.99018$.

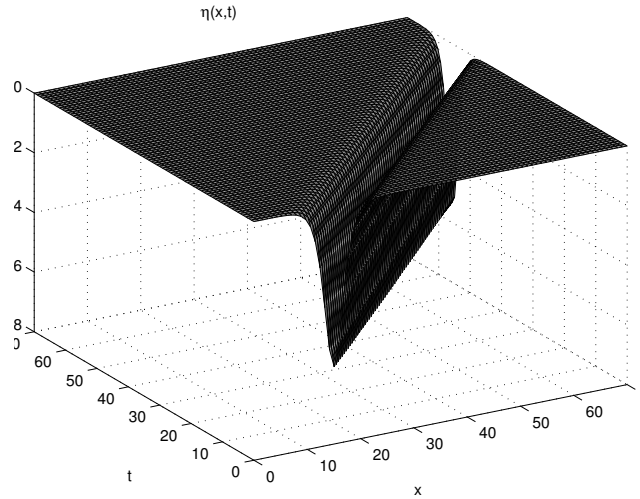

Figure 5: Solitary wave $\eta(x,t)$ as a function of x and t computed by using the numerical scheme. Model's parameters: $\alpha = \beta = 0.01$, $\chi = \pi/8$, $\rho_r = 2.5$, $h = 1$ and the wave speed is $c \approx 0.99018$.

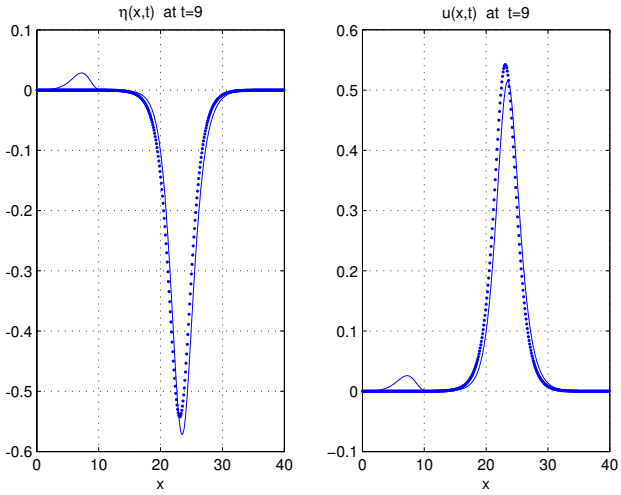

Figure 6: Experiment where the dispersion and nonlinearity are relatively large $\alpha = \beta = 0.1$. Moreover $\chi = \pi/8$, $\rho_r = 2.5$ and $h = 1$. In points: approximate solitary wave (18)-(21). In solid line: solution obtained with the numerical solver. Observe that the approximate solitary wave solution (18)-(21) does not maintain its shape and at time $t = 9$, dispersive and attenuation effects become evident in the profiles of the fluid velocity $U(x,t)$ and the wave elevation $\eta(x,t)$.

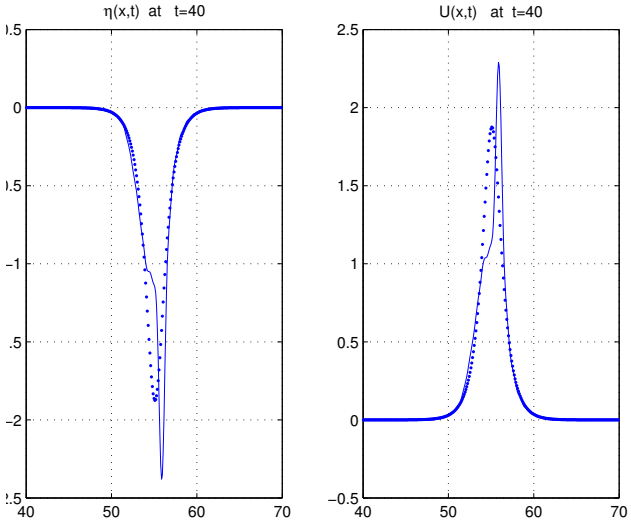

Figure 7: Experiment where the nonlinear parameter is larger than in previous simulations $p = 2$. In points: approximate solitary wave (18)-(21). In solid line: solution obtained with the numerical solver. Model's parameters: $\chi = \pi/3.5$, $\rho_r = 2.5$, $\alpha = \beta = 0.01$, $h = 2$. The numerical parameters are the same than in previous experiments except that $\Delta t = 40/6000$. Observe that the numerical solution does not maintain its shape at time $t = 40$.

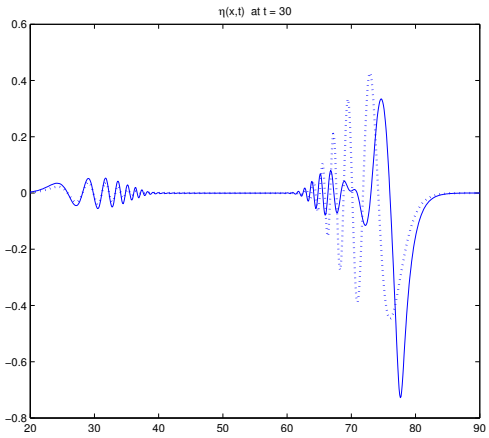

Figure 8: Solution $\eta(x,t)$: Model's parameters: $\rho_r = 2.5$, $\beta = 0.1$, $h = 1$ and $p = 3$. In solid line: nonlinear solution with $\alpha = 0.3$. In dotted line: linear solution.

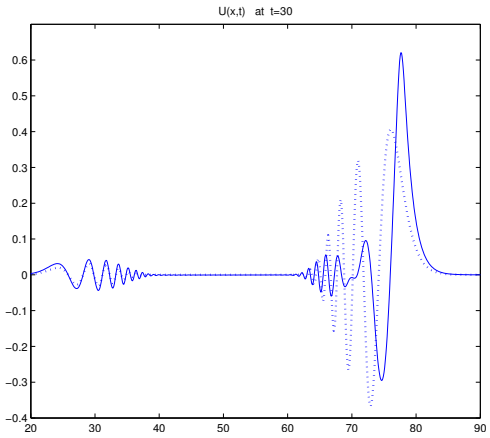

Figure 9: Solution $U(x,t)$: Model's parameters: $\rho_r = 2.5$, $\beta = 0.1$, $h = 1$ and $p = 3$. In solid line: nonlinear solution with $\alpha = 0.3$. In dotted line: linear solution.

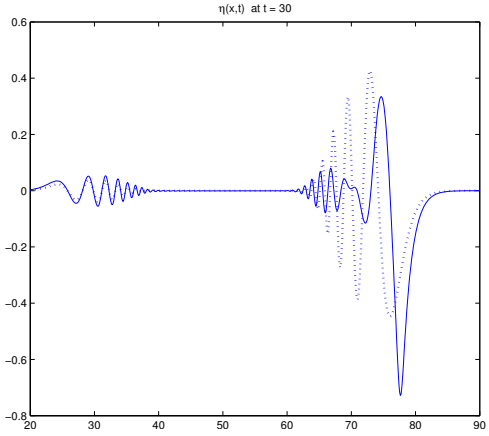

Figure 10: Solution $\eta(x,t)$: Model's parameters: $\rho_r = 2.5$, $\beta = 0.1$, $h = 1$ and $p = 3$. In solid line: nonlinear solution with $\alpha = 0.1$. In dotted line: linear solution.

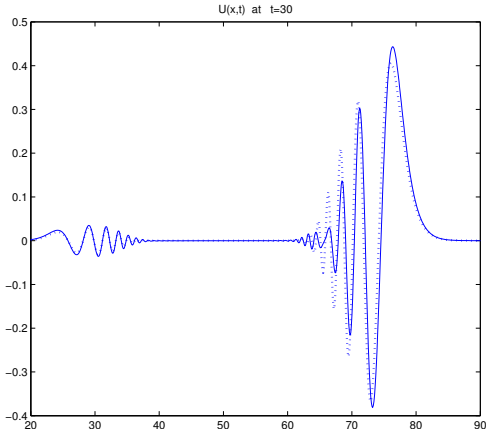

Figure 11: Solution $U(x,t)$: Model's parameters: $\rho_r = 2.5$, $\beta = 0.1$, $h = 1$ and $p = 3$. In solid line: nonlinear solution with $\alpha = 0.1$. In dotted line: linear solution.

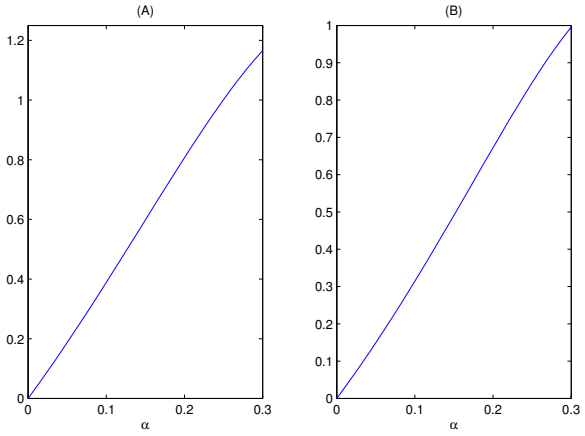

Figure 12: In (A): $||\eta_\alpha - \eta_{linear}||$ at time t=30 as a function of α. In (B): $||U_\alpha - U_{linear}||$ at time t=30 as a function of α. Model's parameters: $\rho_r = 2.5$, $\beta = 0.1$, h=1 and p=3.

seek spatially periodic solutions of system (1)-(2) defined over an interval $[0, L]$ instead of $(-\infty, \infty)$.

To our knowledge it is still an open problem to proof analytically whether solitary-wave solutions exist for $p \geq 1$ and the velocity range where they are factible. On the other hand, it is also necessary to establish theoretically well-posedness of the Cauchy problem associated to system (1)-(2) on periodic and non-periodic spatial domains. These are aspects which we aim to address in a future research.

Acknowledgements The author was supported by the Universidad del Valle under the Project 7738.

References

[1] L. Abdelouhab, J.L. Bona, M. Felland, and J.C. Saut. Nonlocal models for nonlinear, dispersive waves. Physica D 40, pp. 360-392, 1989.

[2] J.P. Albert, J.L. Bona and J.C. Saut. Model equations for waves in stratified fluids. Proc. Royal Soc. Edinburgh Sect. A, 453, pp. 1233-1260, 1997.

[3] E.O. Brigham. The Fast Fourier Transform and its Applications. Prentice Hall, 1988.

[4] W. Choi and R. Camassa. Weakly nonlinear internal waves in a two-fluid system. J. Fluid Mech. 313, pp. 83-103, 1996.

[5] W. Choi and R. Camassa. Fully nonlinear internal waves in a two-fluid system. J. Fluid Mech. 396, pp. 1-36, 1999.

[6] J. Douandikoetxea. Fourier Analysis, (Graduate Studies in Mathematics), American Mathematical Society, 2000.

[7] A.N.W. Hone and V.S. Novikov. On a functional equation related to the intermediate long wave equation. J. Phys. A: Math Gen., 37, no. 32, pp. 399-406, 2004.

[8] R. Joseph. Solitary wave in finite depth fluid. J. Phys. A: Math. Gen. 10, L225-L227, 1977.

[9] Y.S. Kivshar and G. Agrawal. Optical Solitons: From Fibers to Photonic Crystals, Academic Press, 1 Ed., 2003.

[10] T. Kubota, D. Ko and L. Dobbs. Weakly nonlinear internal gravity waves in stratified fluids of finite depth. J. Hydrodynamics 12, pp. 157-165, 1978.

[11] J.N. Pandey. The Hilbert transform of Schwartz distributions and its applications. Wiley-interscience, 1ed., 1995.

[12] B. Pelloni and V.A. Dougalis. Numerical solution of some nonlocal, nonlinear dispersive wave equations. J. Nonlinear Sci. 10, pp. 1-22, 2000.

[13] A. Ruiz and A. Nachbin. A reduced model for internal waves interacting with topography at intermediate depth. Commun. Math. Sci. vol. 6, n.2, pp. 385-396, 2008.

[14] E.M. Stein. Singular integrals and differentiability properties of functions, Princeton University Press, 1971.

Author's address

Juan Carlos Muñoz — Departamento de Matemáticas, Universidad del Valle, Cali, Colombia

e-mail: `jcarlmz@yahoo.com`